

RESEARCH ARTICLE

Comparison of the Transcriptomes of Mouse Skin Derived Precursors (SKPs) and SKP-Derived Fibroblasts (SFBs) by RNA-Seq

Yujie Mao¹, Lidan Xiong¹, Siyu Wang^{1,2}, Jianqiao Zhong^{1,3}, Rongying Zhou¹, Li Li^{1*}

1 Department of Dermatology, West China Hospital, Sichuan University, Chengdu, 610041, China, **2** Department of Dermatology, Sichuan Academy of Medical Sciences and Sichuan Provincial People's Hospital, Chengdu, 610041, China, **3** Department of Dermatology, Affiliated Hospital of Luzhou Medical College, Luzhou, 646000, China

* lili6271@gmail.com



Abstract

Skin-derived precursors (SKPs) from dermis possess the capacities of self-renewal and multipotency. *In vitro* and *in vivo* studies demonstrated that they can differentiate into fibroblasts. However, little is known about the molecular mechanism of the differentiation of SKPs into fibroblasts. Here we compare the transcriptomes of mouse SKPs and SKP-derived fibroblasts (SFBs) by RNA-Seq analysis, trying to find differences in gene expression between the two kinds of cells and then elucidate the candidate genes that may play important roles in the differentiation of SKPs into fibroblasts. A total of 1971 differentially expressed genes (DEGs) were identified by RNA-Seq, which provided abundant data for further analysis. Gene Ontology enrichment analysis revealed that genes related to cell differentiation, cell proliferation, protein binding, transporter activity and membrane were significantly enriched. The most significantly up-regulated genes *Wnt4*, *Wisp2* and *Tsp-1* and down-regulated genes *Slitrk1*, *Klk6*, *Agtr2*, *Ivl*, *Msx1*, *IL15*, *Atp6v0d2*, *Kcne1l* and *Thbs4* may play important roles in the differentiation of SKPs into fibroblasts. KEGG analysis showed that DEGs were significantly enriched in the TGF- β signaling pathway, Wnt signaling pathway and Notch signaling pathway, which have been previously proven to regulate the differentiation and self-renewal of various stem cells. These identified DEGs and pathways could facilitate further investigations of the detailed molecular mechanisms, making it possible to take advantage of the potential therapeutic applications of SKPs in skin regeneration in the future.

OPEN ACCESS

Citation: Mao Y, Xiong L, Wang S, Zhong J, Zhou R, Li L (2015) Comparison of the Transcriptomes of Mouse Skin Derived Precursors (SKPs) and SKP-Derived Fibroblasts (SFBs) by RNA-Seq. PLoS ONE 10(2): e0117739. doi:10.1371/journal.pone.0117739

Academic Editor: Zhi Wei, New Jersey Institute of Technology, UNITED STATES

Received: January 28, 2014

Accepted: December 31, 2014

Published: February 26, 2015

Copyright: © 2015 Mao et al. This is an open access article distributed under the terms of the [Creative Commons Attribution License](http://creativecommons.org/licenses/by/4.0/), which permits unrestricted use, distribution, and reproduction in any medium, provided the original author and source are credited.

Funding: This work was supported by the National Natural Science Foundation of China (81071312), (<http://www.nsf.gov.cn/>). The funders had no role in study design, data collection and analysis, decision to publish, or preparation of the manuscript.

Competing Interests: The authors have declared that no competing interests exist.

Introduction

Recent developments in stem cell biology have generated much excitement about the potential for regenerative medicine and cell-based therapies in a variety of clinical applications, such as treating leukemia, Parkinson's disease and wounds. As skin is easily accessible for autologous

transplantation, stem cells isolated from skin could be promising candidates for prospective therapeutic applications.

Skin-derived precursors (SKPs) from dermis possess the capacities of self-renewal and multipotency [1–2]. They can differentiate into cells of both neural and mesodermal lineages, such as neurons, glias, smooth muscle cells, osteogenic and adipogenic cells [1–5]. It has also been reported that SKPs can differentiate into fibroblasts. When attached onto culture dishes by serum, SKPs initiated differentiation and developed into a fibroblast-like morphology. These SKP-derived fibroblasts (SFBs) could express fibroblast markers fibronectin and vimentin, but did not express SKP marker nestin [6]. *In vivo* experiments demonstrated that SKPs which were transplanted into dermis became morphologically similar to the endogenous fibroblasts at 2–3 weeks post-transplant and expressed dermal fibroblast markers, but did not express markers of neurons or peripheral glia [7–8]. As the predominant cells in dermis, fibroblasts play a pivotal role in maintaining the form and function of skin. The loss or function impairment of fibroblasts is mainly caused by aging or by injury. Given that SKPs can differentiate into fibroblasts, they might be useful for treating aged skin or regenerating skin after damage since they can replenish lost or damaged fibroblasts.

A complex interplay between the intrinsic genetic processes of stem cells and their environment, including the effects of specific cytokines, determines whether they self-renew, remain quiescent, proliferate, differentiate, or undergo apoptosis. Hence, understanding the nature of SKPs and the molecular process by which these cells differentiate into fibroblasts is crucial for the success of cell based therapies. As the phenotype of any given cell is ultimately the product of its genes, it is necessary to identify gene expression of the cells we are interested in, which for the present study are SKPs and SFBs.

RNA-seq is a high-throughput sequencing platform that can be used for discovery and quantification of transcripts in a single experiment [9–12] and reveal differential expression between different samples [13]. Recent studies have shown RNA-seq to be more accurate over a larger dynamic range of gene expression than microarrays [14–15].

No studies performed with mice employing a transcriptome comparison between SKPs and SFBs have been reported. Therefore, the aim of this study is to compare the transcriptomes of mouse SKPs and SFBs by RNA-Seq analysis. Such an analysis would help determine the candidate genes that might play important roles in the differentiation of SKPs into fibroblasts, explain the molecular mechanisms, and then accelerate the therapeutic application of SKPs in skin.

Materials and Methods

Cell Isolation

BALB/c mice at postnatal day 3 for cell isolation were purchased from the Center of Experimental Animal, West China Hospital, Sichuan University. All animal procedures were approved by the Institutional Animal Care and Use Committee of Sichuan University (2013006A). The protocol for isolating SKPs has been described previously in detail [16]. Briefly, dorsal skin was dissected from neonatal BALB/c mice and cut into 2–3 mm² pieces. These dissected pieces were washed three times with Hank's balanced salt solution (Invitrogen, USA) and digested with 0.1% trypsin (Invitrogen, USA) under gentle agitation for 30–50 min at 37°C. When tissue pieces became pale, they were washed three times, once with wash medium (DMEM/F12(3:1) (Invitrogen, USA) containing 1% penicillin/streptomycin (Cambrex, USA)) plus 10% fetal bovine serum and twice with Hank's balanced salt solution. The epidermis was then removed from the dermis. Afterwards, dermis pieces were digested by collagenase type XI (Sigma-Aldrich, USA) for one hour at 37°C, mechanically dissociated with scissors and

subsequently triturated repeatedly in wash medium with a 1000 μ l pipette tip. The supernatant was collected and the trituration was repeated until tissue pieces became thin. After the dissociated cell suspension was filtered through a 40 μ m cell strainer and centrifuged at 1200 rpm for 7 min, the pellet was suspended in proliferation medium (DMEM/F12(3:1) containing 0.1% penicillin/streptomycin, 40 ng/ml FGF2 (Collaborative, USA), 20 ng/ml EGF (Collaborative, USA) and 2% B27 supplement (Invitrogen, USA)) to an optimum density of 10000–30000 cells/ml of medium. Finally, cells were cultured in proliferation medium at 37°C and used for experiments at the second generation. Cells were passaged every 3–4 days and used for experiments at the second generation. Primary fibroblasts (PFBs) were isolated from the dermis of neonatal BALB/c mice and cultured in DMEM plus 10% fetal bovine serum.

Induction of Differentiation

For the induction of SKP differentiation into SFBs, SKP spheres were collected and suspended in DMEM plus 10% fetal bovine serum, and then plated onto a cell culture dish (Corning, USA) whose surface was coated with poly-L-lysine (Sigma-Aldrich, USA).

Immunocytochemistry

Cells were fixed by 4% paraformaldehyde. The fixed cells were blocked with 3% BSA for 30 min and subsequently incubated with primary antibody overnight at 4°C. After washing with PBS 3 times, they were incubated with secondary antibody for 1 h at room temperature. Finally they were incubated with DAPI for 1 min. A parallel culture with secondary antibody only was employed as a negative control, a culture without any antibody was used as a blank control. Primary antibodies were monoclonal anti-fibronectin (Abcam, UK, 1:250), monoclonal anti-vimentin (Abcam, UK, 1:200), monoclonal anti-nestin (Abcam, UK, 1:500), monoclonal anti-SOX2 (Abcam, UK, 1:200) and polyclonal anti-collagen 1 (Abcam, UK, 1:500). Secondary antibodies were Alexa Fluor 488 goat-rabbit, Alexa Fluor 555 goat-rabbit and Alexa Fluor 488 goat-mouse (Invitrogen, USA, 1:500). The preceding protocol was performed in triplicate for each cell type described.

RNA-Seq

Library Preparation. cDNA library preparation was performed at BGI-Shenzhen. The total RNA from SKPs and SFBs were firstly treated with DNase I to degrade contaminating DNA. mRNA was enriched by using oligo(dT) magnetic beads. The mRNA was broken into short fragments (about 200 bp) in fragmentation buffer. The RNA fragments were then ligated to adaptors and converted into cDNA, which was purified using magnetic beads. End reparation and 3'-end single nucleotide A (adenine) addition was then performed. Finally, sequencing adaptors were ligated to the fragments. The resulting fragments were enriched by PCR amplification. The library products were used for sequencing using Illumina HiSeqTM 2000. SKPs were considered as the control and SFBs were the treatment.

Mapping Reads to the Reference Genome. The original image data produced by the sequencer was transferred into sequences using base calling. These sequences were defined as "raw reads". Prior to mapping these reads to the reference database, all sequences were filtered to remove adaptor sequences, N sequences (in which the percentage of unknown bases (N) was greater than 10%) and low-quality sequences (the percentages of low quality bases with a quality value ≤ 5 was greater than 50% in a read). The remaining reads were mapped to the mouse genome using SOAPaligner/SOAP2 [17]. No more than 2 mismatches were allowed in the alignment.

Normalized Expression Levels of Genes and Screening of Differentially expressed genes (DEGs). The gene expression level was calculated by using RPKM [10] method (Reads Per Kb per Million reads). The used formula was as follows:

$$RPKM(A) = \frac{10^6 C}{NL/10^3}$$

RPKM(A) is the expression level of gene A, C is the number of reads that uniquely aligned to gene A, N is the total number of reads that uniquely aligned to all genes, and L is the number of bases of gene A. The RPKM method is able to eliminate the influence of different gene length and sequencing discrepancies on the calculation of gene expression levels. Therefore, the RPKM values could be directly used for comparing the difference of gene expression among samples. The cutoff value for determining gene transcriptional activity was determined based on a 95% confidence interval for all RPKM values for each gene. A strict algorithm had been developed to identify DEGs between two samples based on “The significance of digital gene expression profiles” [18]. We used a P-value corresponding to a differential gene expression test at statistically significant levels [19]. “FDR(False Discovery Rate) ≤ 0.001 and the absolute value of $\log_2\text{Ratio} \geq 1$ ” were used to identify DEGs as the threshold.

Gene Ontology(GO) and KEGG Pathway Enrichment Analysis of DEGs. GO enrichment analysis provides all GO terms that are significantly enriched in DEGs compared to the genome background, and filters the DEGs that correspond to biological functions. This method maps all DEGs to GO terms in the database (<http://www.geneontology.org/>), calculates gene numbers for every term, then uses hypergeometric test to find significantly enriched GO terms in DEGs compared to the genome background. The calculating formula is:

$$P = 1 - \sum_{i=0}^{m-1} \frac{\binom{M}{i} \binom{N-M}{n-i}}{\binom{N}{n}}$$

N is the number of all genes with GO annotation, n is the number of DEGs in N, M is the number of all genes that are annotated to the certain GO terms, m is the number of DEGs in M. The calculated p-value went through Bonferroni Correction, using a corrected p-value ≤ 0.05 as a threshold. GO annotation of DEGs was carried out using the Blast2GO program. After getting GO annotation for DEGs, we used WEGO software [20] to do GO functional classification for DEGs and to understand the distribution of gene functions of the species from the macro level. For KEGG annotation, which is the major public pathway-related database [21], the calculating formula is the same as that in GO analysis, where N is the number of all genes, n is the number of DEGs in N, M is the number of all genes annotated to specific pathways, and m was the number of DEGs in M.

Software and Databases. The software and databases used to analyze the RNA-Seq data are shown in [Table 1](#).

Real Time Quantitative Reverse Transcription PCR(qRT-PCR)

Main DEGs involved in cell differentiation and important signaling pathways were selected: *Bmp2*, *Kit*, *Id2*, *Bnc1*, *Wnt2b*, *Ptch2*, *Actg2*, *Wnt4*, *Myh11*, *Acta2*, *Smad6*, *Smad9*, *Myc*, *Megf6*, *Dner*, *Slitrk1*, *Lvl*, *Klk6*, *Agtr2*, *Tgfbr1*, *Smad3*, *Wnt11*, *Fzd10*, *Fzd4*, *Jun*, *Notch4*, *Notch1*, *Dlk1*, *Dtx4*. Total RNA was extracted using the RNeasy micro kit (Qiagen, Germany) and then was converted to cDNA using the SuperScript II Reverse Transcriptase kit (Invitrogen, USA)

Table 1. Software and Databases.

Analysis	Software/Algorithm (Version)	Database (Version)
Statistics of alignment	Soap(2.21)	
Functional annotation	BLAST(2.2.23); Blast2GO(2.2.5)	KEGG(updated monthly if possible); NR(updated monthly if possible); GO(updated monthly if possible)
Quantification of gene expression	RPKM algorithm	
Screening of DEGs	Poisson distribution model	
Expression pattern analysis	Cluster(3.0); Java Tree View (1.1.6r2)	
Gene Ontology enrichment analysis	Hypergeometric distribution model	GO(updated monthly if possible)
Pathway enrichment analysis	Hypergeometric distribution model	KEGG(updated monthly if possible)

doi:10.1371/journal.pone.0117739.t001

according to the manufacturer’s protocol. qRT-PCR was performed using a StepOnePlus Real-Time PCR System(Applied Biosystems) with Taqman primer/probe sets from Applied Biosystems. Three independent biological and two technical replicates were performed. mRNA expression levels were normalized by the internal β -actin control and then represented as the log₂ ratio of the normalized values in fibroblasts to those in SKPs. Pearson correlation coefficient between qRT-PCR data and RNA-Seq data was calculated to validate RNA-Seq experiments. *T*-test was used to compare the gene expression between SFBs and PFBs and *P* < 0.01 was considered to be statistically significant.

Results

Differentiation of SKPs into Fibroblasts

SKPs were successfully isolated from mouse dermal tissue and showed sphere-like structure in the suspension culture(Fig. 1A). SKPs attached to the bottom of poly-L-lysine treated dishes and exhibited fibroblast-like morphology(Fig. 1B and C) 3 days after serum induction. Consistent with previous studies [1, 8], SKP spheres expressed SOX2(Fig. 2A), nestin(Fig. 2D), vimentin(Fig. 2G) and fibronectin(Fig. 2I) when measured by immunocytochemistry. SFBs expressed fibroblast markers vimentin(Fig. 2I), fibronectin(Fig. 2L) and collagen 1(Fig. 2O), but did not express SOX2(Fig. 2C) or nestin(Fig. 2F). The same result was observed with PFBs(Fig. 2B, E,

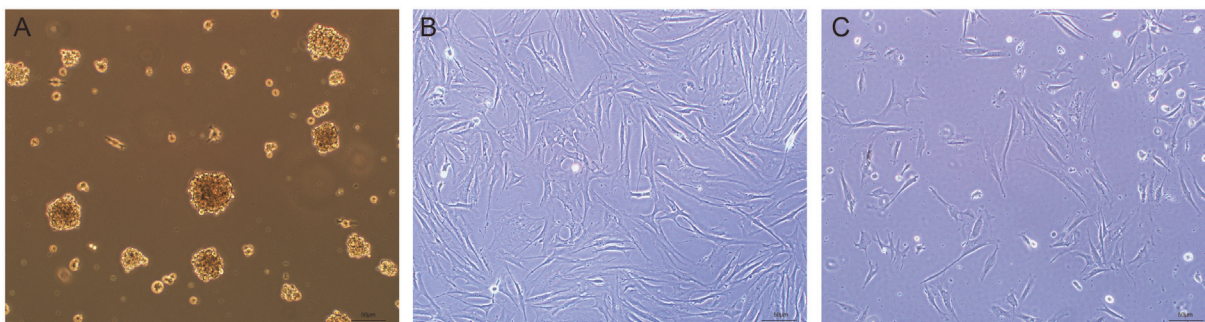


Fig 1. Morphology of SKPs and fibroblasts. (A) SKPs exhibited sphere-like structure in suspension culture.(B) PFBs were typically stellate or spindle shaped.(C) SFBs had the same morphology as PFBs.

doi:10.1371/journal.pone.0117739.g001

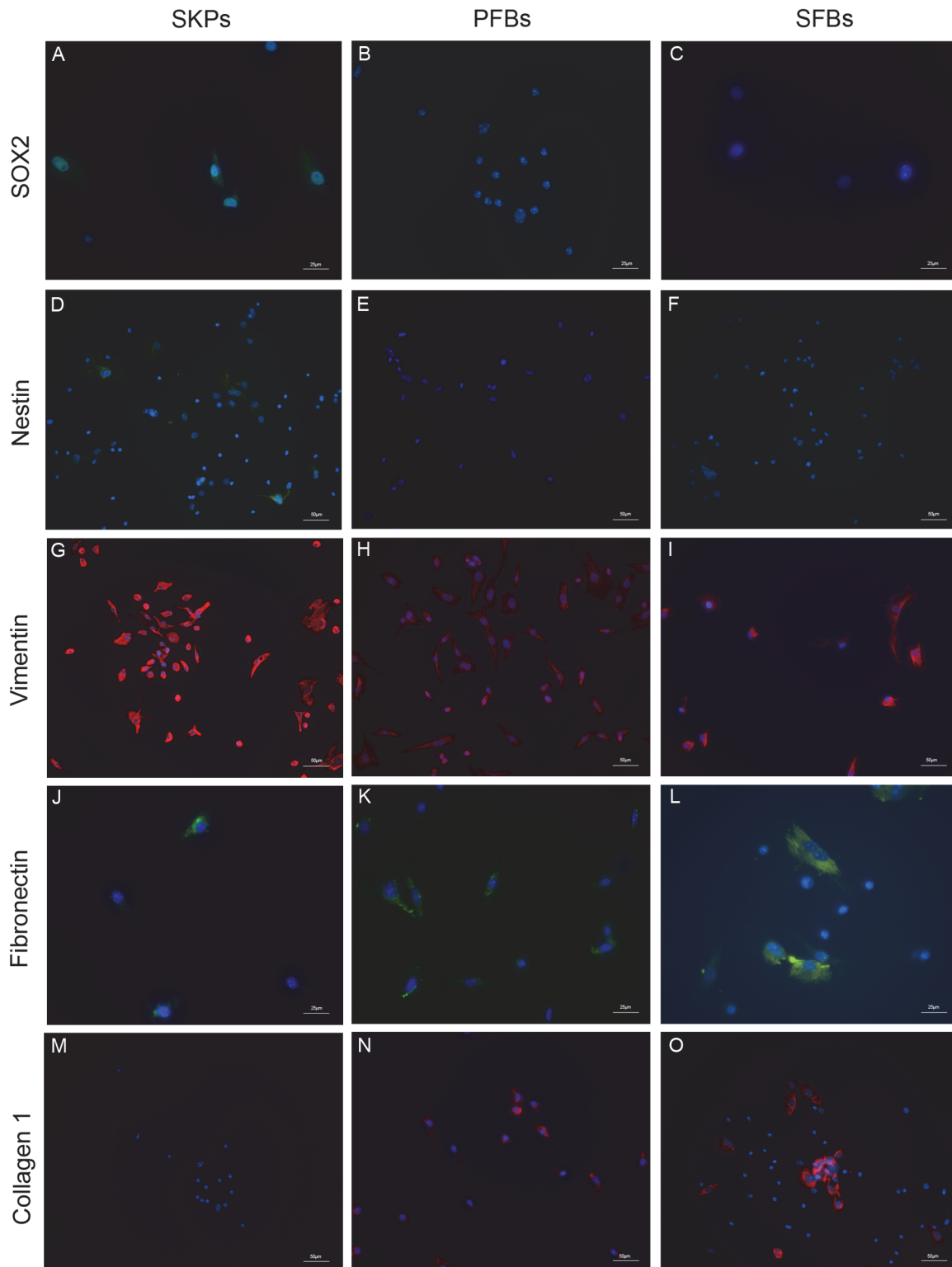


Fig 2. Characterization of SKPs and SFBs by immunocytochemistry. SKP spheres expressed SOX2(A), nestin(D), vimentin(G) and fibronectin(J), did not express collagen 1 (M); SFBs expressed vimentin(I), fibronectin(L) and collagen 1 (O), did not express SOX2(C) or nestin(F). The same results were observed with PFBS(B, E, H, K and N). Scale bars, 25 μm(A-C, J-L); 50 μm(D-I, M-O).

doi:10.1371/journal.pone.0117739.g002

H, K and N). These results showed that SKPs could differentiate into fibroblasts, which is consistent with previous studies [6–8].

Quality Assessment of Reads and Statistics of Alignment

To try to look into potential regulatory mechanisms that drive SKPs differentiate to SFBs, we performed RNA-Seq to measure RNA profiles in SKPs and SFBs. More than 20 million raw reads were generated from the SKPs or SFBs library. After filtering the only adaptor sequences, those containing N sequences and low quality sequences, the two RNA-Seq libraries still generated over 19 million clean reads from each library. The percentage of clean reads among raw tags in each library ranged from 95.95% to 98.38% (Fig. 3). Of the total reads, more than 84% matched to the mouse genome. The remaining sequences were unmatched (Table 2), because only reads aligning entirely inside exonic regions could be matched (reads from exon-exon junction regions could not be matched).

Analysis of DEGs of SKPs and SFBs

A total of 1971 genes were differentially expressed between SKPs and SFBs, with 747 genes up-regulated and 1224 down-regulated (Fig. 4).

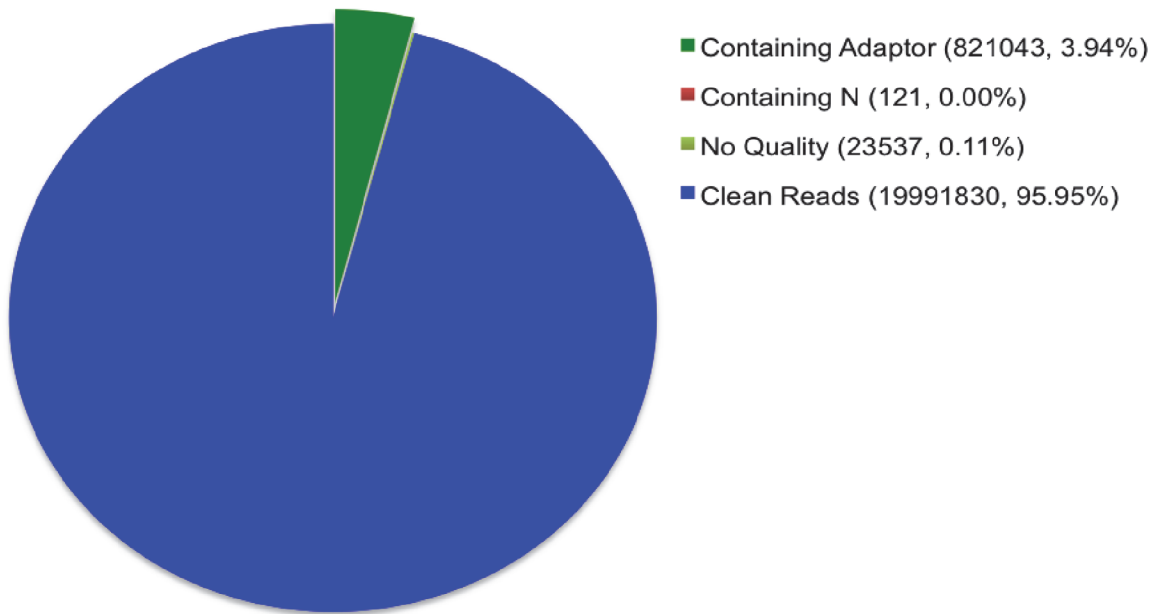
GO and KEGG pathway Enrichment Analysis of DEGs

GO is an international standardized gene functional classification system which offers a dynamic-updated controlled vocabulary and a strictly defined concept to comprehensively describe properties of genes and their products in any organism. GO covers three domains: cellular component, molecular function and biological process. The basic unit of GO is GO-term. Every GO-term belongs to a type of ontology. GO enrichment analysis provides all GO terms that are significantly enriched in DEGs compared to the genome background, and filters the DEGs that correspond to biological functions. In this study, 1971 DEGs could be categorized into 51 functional groups (Fig. 5). In the three main domains (biological process, cellular component and molecular function) of the GO classification, 28, 10 and 13 functional groups were identified, respectively. Among these groups, the terms cellular process, metabolic process and regulation of biological process in the biological process, the cell, cell part and organelle in the cellular component, the binding, catalytic activity and molecular transducer activity in the molecular function were dominant. Genes related to cell differentiation, cell proliferation, protein binding, transporter activity and membrane were also significantly enriched. The top five most up-regulated and down-regulated genes involved in these terms are listed in Table 3. Genes usually interact with each other to play roles in certain biological functions. Pathway-based analysis helps to further understand DEGs biological functions. KEGG pathway enrichment analysis identifies significantly enriched metabolic pathways or signal transduction pathways in DEGs compared with the whole genome background. 51 pathways were identified to be significantly enriched in DEGs between SKPs and SFBs (S1 Table). The most widely reported pathways related to stem cell pluripotency and differentiation, such as the TGF- β signaling pathway (S1 Fig.), Wnt signaling pathway (S2 Fig.) and Notch signaling pathway (S3 Fig.) were all included. The main DEGs involved in these signaling pathways are listed in Table 4.

qRT-PCR for Data Validation

Main DEGs involved in cell differentiation and important signaling pathways were selected to verify the RNA-seq data by qRT-PCR. Pearson correlation coefficient between qRT-PCR data and RNA-Seq data was 0.960, which indicates that the RNA-Seq data is highly correlated with

Composition of Raw Reads (SKP_RNA)



Composition of Raw Reads (SFB_RNA)

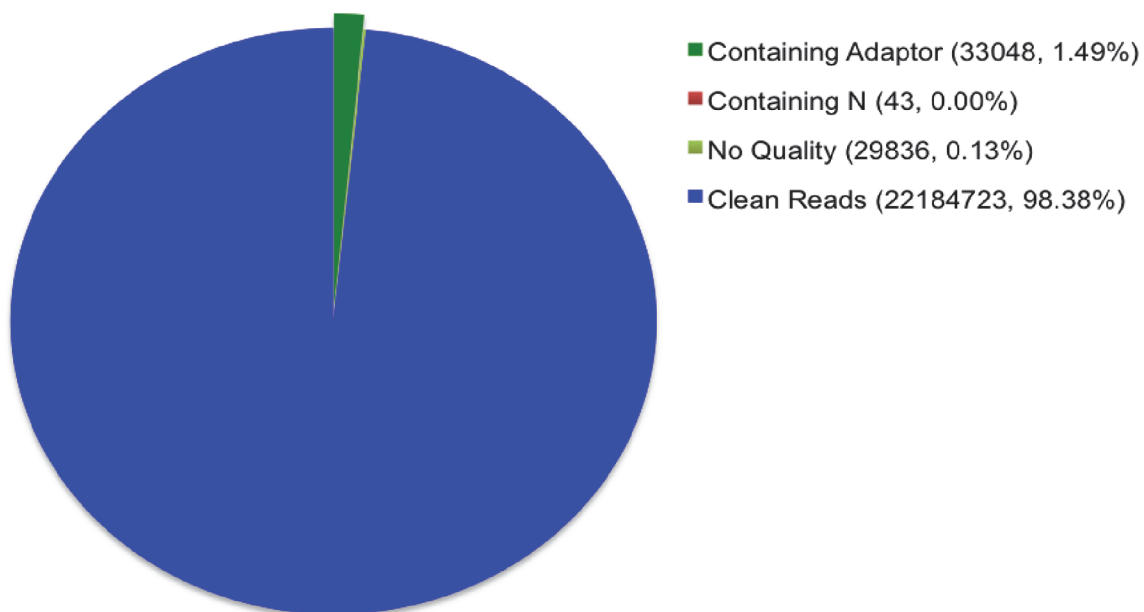


Fig 3. Classification of total raw reads. After filtering the only adaptor sequences, containing N sequences and low quality sequences, the RNA-Seq libraries of SKPs and SFBs generated over 19 million clean reads each, and the percentage of clean reads among raw tags in each library ranged from 95.95% to 98.38%.

doi:10.1371/journal.pone.0117739.g003

Table 2. Summary of mapping results(mapping to reference genes).

Sample ID	Total Reads	Total Base Pairs	Total Mapped Reads	Perfect Match	< = 2bp Mismatch	Unique Match	Multi-position Match	Total Unmapped Reads
FB_RNA	22184723 (100.00%)	1087051427 (100.00%)	18688411 (84.24%)	15753372 (71.01%)	2935039 (13.23%)	14105047 (63.58%)	4583364 (20.66%)	3496312(15.76%)
SKP_RNA	19991830 (100.00%)	979599327 (100.00%)	17234956 (86.21%%)	14226186 (71.16%)	3008770 (15.05%)	12832756 (64.19%)	4402201 (22.02%)	2756873(13.79%)

doi:10.1371/journal.pone.0117739.t002

the qRT-PCR data(Fig. 6). PFBs were also tested by qRT-PCR. There was no significant difference in the expression of candidate genes between SFBs and PFBs except *Dlk1*(Fig. 7). Although the expression level of *Dlk1* between SFBs and PFBs was significantly different by qRT-PCR, it was down-regulated when compared with SKPs, which was consistent with the results from RNA-Seq. These results confirmed that RNA-Seq could provide reliable data for mRNA differential expression analysis.

Discussion

In this study we compared the transcriptional profiles of mouse SKPs and SFBs by RNA-Seq. Up to 1971 genes were found to be significantly differentially expressed, which was a much larger number than the finding by microarray [6]. The results suggest that RNA-Seq is a very

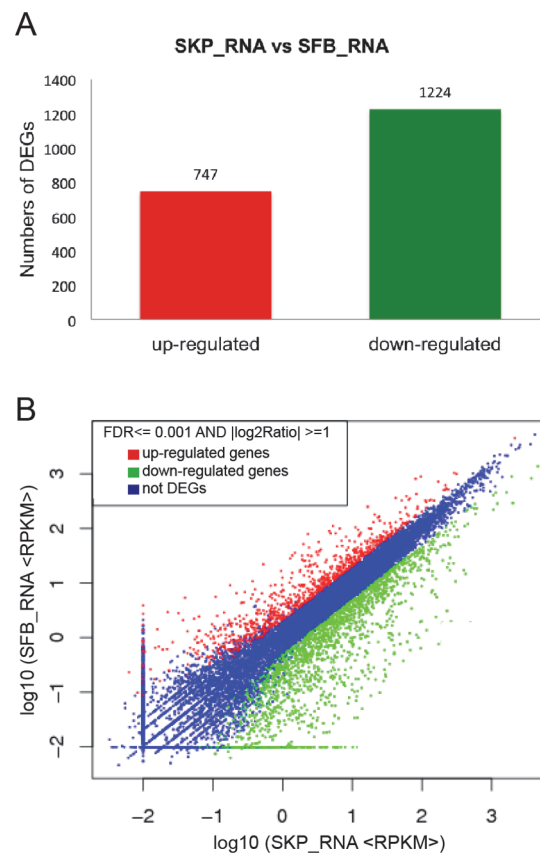


Fig 4. DEGs between SKPs and SFBs. (A) The numbers of DEGs.(B) Scattered plot of DEGs.

doi:10.1371/journal.pone.0117739.g004

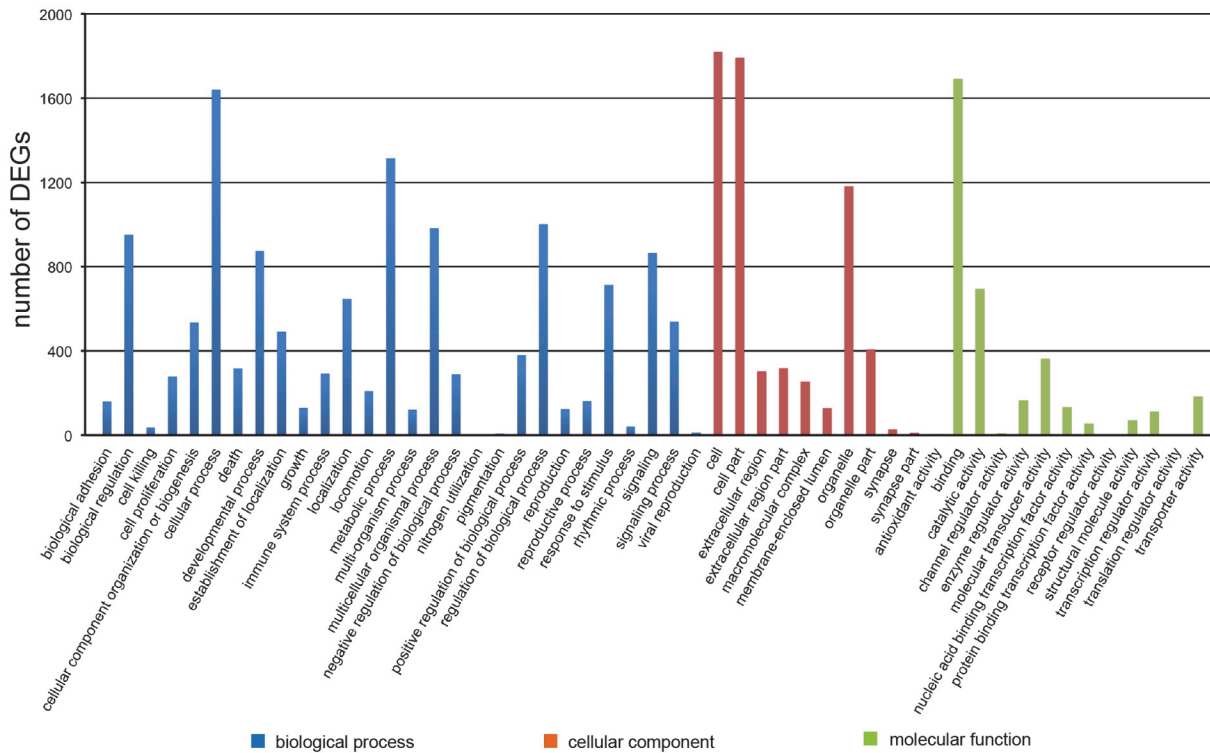


Fig 5. GO functional classification(WEGO) of DEGs. The results were summarized in three main domains: biological process, cellular component and molecular function. In the three main domains, 28, 10 and 13 functional groups were identified respectively.

doi:10.1371/journal.pone.0117739.g005

sensitive tool to compare the gene expression between cells. GO analysis of the DEGs showed that these DEGs were significantly enriched in cell membrane and in the process of cell differentiation, cell proliferation, protein binding and transporter activity. Analysis of DEGs that are significantly enriched and involved in the above terms could help us identify the important candidate genes which might play important roles in the transition from SKPs to fibroblasts. Analysis of genes coding for cell membrane may also help us find the surface makers of SKPs and fibroblasts.

Among the listed up-regulated genes in [table 3](#), the genes which encode WNT4 and WISP2 are both evidence of Wnt signaling activation [22–23]. The up-regulation of *Wnt4* and *Wisp2* indicates that the activation of the Wnt signaling pathway plays an important role in the transition from SKPs to fibroblasts. Thrombospondin-1(TSP-1), from the cell proliferation term, is

Table 3. Most up-regulated and down-regulated genes involved in important terms about stem cells.

Term	Up-regulated genes	Down-regulated genes
cell differentiation	<i>Actg2, Wnt4, Myh11, Acta2, Tspan2</i>	<i>Slitrk1, Steap4, Ivl, Klk6, Agtr2</i>
cell proliferation	<i>Wisp2, Adra1d, Myocd, Thbs1, Tnfrsf11a</i>	<i>Camp, Thbs4, Msx1, Ace, IL15</i>
protein binding	<i>Wisp2, Myh11, Npas4, Wnt4, Cnn1</i>	<i>Lcn2, Thbs4, Stfa3, Agtr2, Sprr1b</i>
transporter activity	<i>Gabra4, Trpc6, Accn3, Slc13a5, Lrp2</i>	<i>Slc14a1, Atp6v0d2, Kcne1l, Clic5, Dmrt2</i>
membrane	<i>Slc13a5, Gal3st1, Wnt4, Lrp2, Adra1d</i>	<i>S100a8, Slitrk1, Atp6v0d2, Cd79b, Cidec</i>

doi:10.1371/journal.pone.0117739.t003

Table 4. List of possible signaling pathways and major DEGs involved in these pathways.

Signaling pathway	Up-regulated DEGs	Down-regulated DEGs
TGF-β signaling pathway	<i>Gdf6, Tgfb3, Inhb, Bmpr2, Acvr2a, Smad6/9, Myc, Id3/4</i>	<i>Bmp2/4/6/7, Bmpr1, Tgfb1, Tgfb1, Smad3, Cdkn2, Id2</i>
Wnt signaling pathway	<i>Wnt4, Wnt2b, Wnt9a, C-myc</i>	<i>Wnt7b, Wnt2, Wnt6, Wnt11, Fzd10, Fzd4, C-jun, Fra-1, Cyc-d</i>
Notch signaling pathway	<i>Megf6, Dner</i>	<i>Dlk1, Notch4, Sned1, Megf11, Notch3, Notch1, Notch2, Dtx1, Dtx4, Rbpj</i>

doi:10.1371/journal.pone.0117739.t004

an endogenous activator of TGF- β . TSP-1 has been reported to increase and decrease in parallel with that of TGF- β 1 and collagen III [24]. TSP-1 also activates protein kinase B and decreases apoptotic signaling in suspended fibroblasts [25]. The up-regulation of the gene *Tsp1* indicates that it might help in inducing SKPs to differentiate into fibroblasts through the TGF- β signaling pathway by increasing the proliferation of SKPs.

Among the listed down-regulated genes, *Ivl* is related to epidermal cell differentiation and the protein encoded by it is synthesized in abundance during terminal differentiation of keratinocytes. *ATP6V0D2* has been shown to be a regulator of osteoclast fusion and bone formation. The knock out of *Atp6v0d2* resulted in impaired osteoclast fusion and increased bone formation [26]. The down-regulation of these genes is related to keratinocytes and osteocytes, which indicates that the transition from SKPs to fibroblasts needs the inhibition of the genes that could lead to the differentiation to other cells. Many down-regulated genes have been reported to encode for functions in the neural system. The *Msx1* homeobox gene is expressed at diverse sites of epithelial-mesenchymal interaction during vertebrate embryogenesis, and has been implicated in signaling processes between tissue layers. It has a critical role in mediating epithelial-mesenchymal interactions during craniofacial bone and tooth development [27]. The down-regulation of *Msx1* may increase mesenchymal differentiation. *Slitrk1* encodes a transmembrane protein containing leucine-rich repeats that is produced predominantly in the nervous system. Previous work has shown that *Slitrk1*-deficient mice display elevated anxiety-like behavior and noradrenergic abnormalities [28]. *KLK6* plays a functional role in oligodendrocyte development and the expression of myelin proteins [29]. *AGTR2* regulates central nervous system functions, including behavior [30]. It also plays a role in the central nervous system and cardiovascular functions that are mediated by the renin-angiotensin system [31]. *IL-15* is reported to be a key regulator of neurogenesis in the adult and is essential to understanding diseases with an inflammatory component [32]. The expression pattern of mouse *Kcne1l* in the developing embryo revealed a strong signal in ganglia, in the migrating neural crest cells of cranial nerves, in the somites, and in the myoepicardial layer of the heart. It was reported that *KCNE1L* could be involved in the development of some neurological signs observed in patients with AMME contiguous gene syndrome [33]. Inhibiting the expression of the down-regulated genes which encode the above proteins, which are related to the neural system, may induce SKPs to differentiate into mesodermal lineages rather than neural cells. Notch modulator *THBS4* helps in rodent subventricular zone astrogenesis following injury [34]. The down-regulation of *Thbs4* suggests that the inhibition of the Notch signaling pathway may be involved in the process of transition from SKPs to fibroblasts.

Integration of extrinsic signals, epigenetic regulators, and intrinsic transcription factors underlies the capacity of stem cells to undergo differentiation. Differentiation is controlled by complex signaling networks. KEGG analysis of the DEGs showed that the major developmental signaling pathways including TGF- β signaling pathway, Wnt signaling pathway and Notch

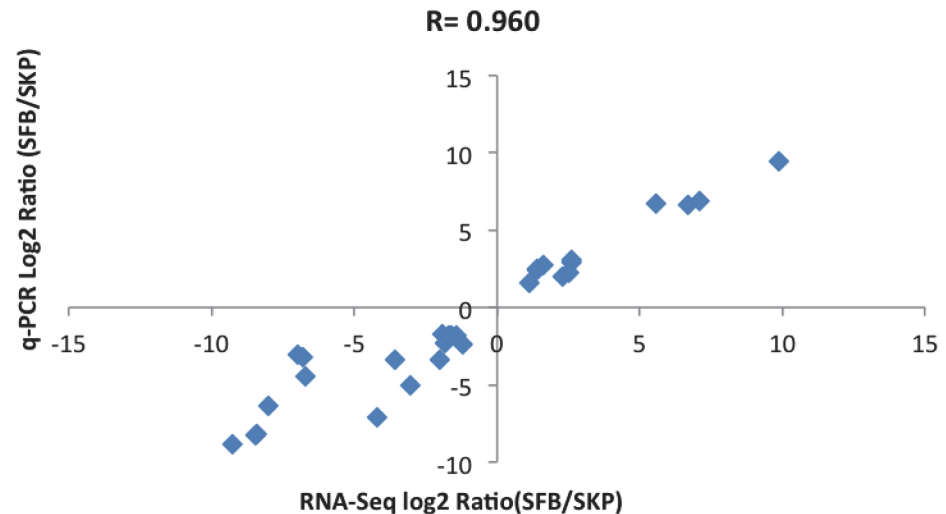


Fig 6. Correlation between RNA-Seq and qRT-PCR data of selected genes. Pearson correlation coefficient ($r = 0.960$) was used to determine the similarity in gene expression pattern between RNA-Seq and qRT-PCR.

doi:10.1371/journal.pone.0117739.g006

signaling pathway were all significantly enriched. These pathways were reported to be involved in the pluripotency and self-renewal of various stem cells.

The TGF- β signaling pathway is a series of molecular signals initiated by the binding of an extracellular ligand to a TGF- β receptor on the surface of a target cell, and ending with regulation of a downstream cellular process. The TGF- β superfamily comprises nearly 30 growth and differentiation factors that include TGF- β s, activins, inhibins, and bone morphogenetic proteins (BMPs). TGF- β inhibits proliferation of multipotent hematopoietic progenitors and promotes lineage commitment of neural precursors. BMPs block neural differentiation of mouse and human embryonic stem cells (ESCs) [35]. The TGF- β signaling pathway takes part in the differentiation process of various stem cells. Master differentiation genes in ESCs are sequestered by repressive chromatin marks. TRIM33-Smad2/3 and Smad4-Smad2/3 complexes mediated TGF- β signals enable the transcriptional activation of ESCs [36]. Small interfering RNA experiments proved that TGF- β 1 signaling through Smad2 and Smad3 plays an important role in the development of smooth muscle cells from totipotent ESCs [37]. TGF- β 1 also suppresses ESC chondrogenic induction [38]. Canonical TGF- β signaling via Smad4 regulates the balance between proliferation and differentiation of neural stem cells in the midbrain [39]. The activation of TGF- β /BMP signaling pathway drives mesenchymal stem cells to differentiate into osteoblasts [40]. It also plays a crucial role in osteoblast differentiation of the adipose-derived stem cells. The members which are involved in the process include Smad 1, Smad5, Smad8, P38, ASK1, MKK3, MKK6, Runx2, collagen type 1, and osteopontin [41]. The TGF- β signaling pathway regulates the differentiation and proliferation of stem cells in different stages. In this study, The down-regulation of the gene *Smad3* led to up-regulation of transcription factors MYC and down-regulation of CDKN2 and ID2, which may be important in the differentiation from SKPs to fibroblasts. The Wnt signaling pathway was also reported to regulate the proliferation and differentiation of embryonic stem cells [42] and various kinds of adult stem cells [43–46]. In the Wnt signaling pathway, the up-regulated ligands WNT7B, WNT2, WNT6, WNT11 and the down-regulated WNT4 and WNT2B bound to their receptors, and led to the up-regulation of *C-myc* and down-regulation of *C-jun*, *Fra-1* and *Cyc-d*, which might also contribute to the differentiation of SKPs into fibroblasts. Notch signaling exhibits dynamic

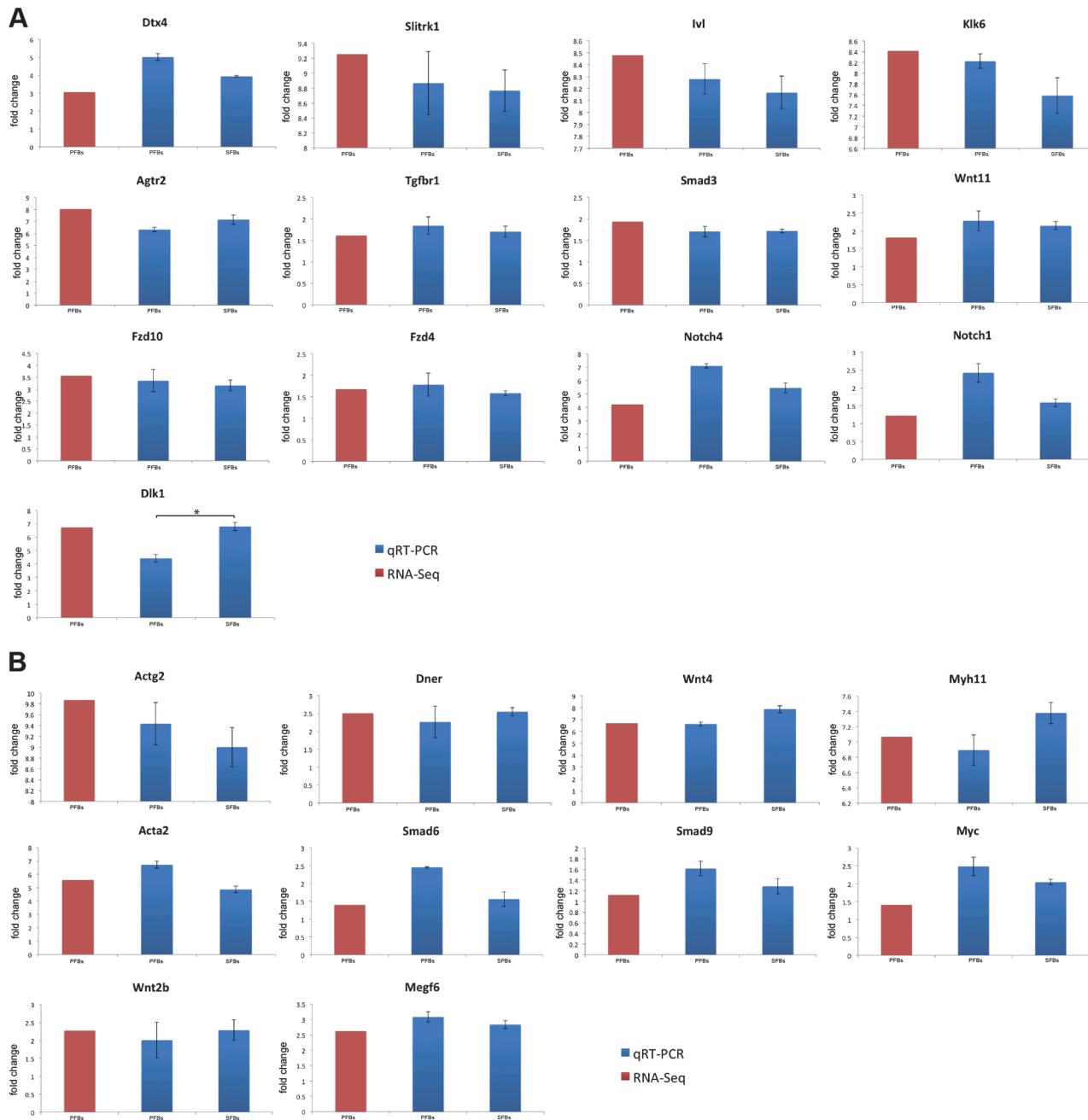


Fig 7. Validation of RNA-Seq results and comparison of gene expression between SFBs and PFBs by qRT-PCR. (A) Down-regulated genes. (B) Up-regulated genes. Fold changes shown are ((SFBs or PFBs gene expression level)/(SKPs gene expression level)). Error bars represent SE; * represents statistically significant.

doi:10.1371/journal.pone.0117739.g007

expression characteristics in bone marrow-derived mesenchymal stem cells during the process of differentiation into hepatocytes. It was found to be necessary to initiate differentiation into hepatocytes, but must be down-regulated for the differentiation to proceed continuously [47]. It has been shown that low adipogenic clones had significantly higher mRNA expression levels of *Notch2*, *Notch3* and *Notch4*, *Jagged1*, as well as *Delta1*, compared with those of high adipogenic clones. This indicated that the activation of Notch signaling inhibited the adipogenic

differentiation of adipose-derived mesenchymal stem cell clones [48]. Most of the DEGs involved in the Notch signaling pathway, including the genes encoding ligands, receptors and transcription factors, were down-regulated. These data suggest that the Notch signaling pathway plays an important role in keeping SKPs quiescent and the inhibition of this signaling pathway may activate SKPs to differentiate.

In conclusion, we compared the transcriptional profiles between SKPs and SFBs by RNA-Seq. GO analysis of the DEGs showed that the significantly up-regulated genes *Wnt4*, *Wisp2* and *Tsp-1* and the significantly down-regulated genes *Slitrk1*, *Klk6*, *Agtr2*, *Ivl*, *Msx1*, *IL15*, *Atp6v0d2*, *Kcne1l* and *Thbs4* might play important roles in the transition of SKPs to fibroblasts. KEGG analysis showed that DEGs were significantly enriched in the TGF- β signaling pathway, Wnt signaling pathway and Notch signaling pathway, which have been previously shown to regulate the differentiation and self-renewal of various stem cells. These identified DEGs and pathways could facilitate further investigations of the detailed molecular mechanisms, making it possible to take advantage of the potential therapeutic applications of SKPs in skin regeneration.

Supporting Information

S1 Fig. The detailed information of TGF- β signaling pathway. Up-regulated genes are marked with red borders and down-regulated genes with green borders.
(TIF)

S2 Fig. The detailed information of Wnt signaling pathway. Up-regulated genes are marked with red borders and down-regulated genes with green borders.
(TIF)

S3 Fig. The detailed information of Notch signaling pathway. Up-regulated genes are marked with red borders and down-regulated genes with green borders.
(TIF)

S1 Table. KEGG pathway enrichment analysis of DEGs.
(DOCX)

Author Contributions

Conceived and designed the experiments: YM LL. Performed the experiments: YM LX RZ. Analyzed the data: YM. Contributed reagents/materials/analysis tools: SW JZ. Wrote the paper: YM LL.

References

1. Toma JG, Akhavan M, Fernandes KJ, Barnabé-Heider F, Sadikot A, et al(2001) Isolation of multipotent adult stem cells from the dermis of mammalian skin. *Nat Cell Biol* 3: 778–784. PMID: [11533656](#)
2. Kang HK, Min SK, Jung SY, Jung K, Jang da H, et al(2011) The potential of mouse skin-derived precursors to differentiate into mesenchymal and neural lineages and their application to osteogenic induction *in vivo*. *Int J Mol Med* 28: 1001–1011. doi: [10.3892/ijmm.2011.785](#) PMID: [21879252](#)
3. Dyce PW, Zhu H, Craig J, Li J(2004) Stem cells with multilineage potential derived from porcine skin. *Biochem Biophys Res Commun* 316: 651–658. PMID: [15033449](#)
4. Fernandes KJ, McKenzie IA, Mill P, Smith KM, Akhavan M, et al(2004) A dermal niche for multipotent adult skin-derived precursor cells. *Nat Cell Biol* 6: 1082–1093. PMID: [15517002](#)
5. Zhao M, Isom SC, Lin H, Hao Y, Zhang Y, et al(2009) Tracing the stemness of porcine skin-derived progenitors(pSKP) back to specific marker gene expression. *Cloning Stem Cells* 11: 111–122. doi: [10.1089/clo.2008.0071](#) PMID: [19226215](#)

6. Zhao MT, Whitworth KM, Zhang X, Zhao J, Miao YL, et al(2010) Deciphering the mesodermal potency of porcine skin-derived progenitors(SKP) by microarray analysis. *Cell Reprogram* 12: 161–173. doi: [10.1089/cell.2009.0060](https://doi.org/10.1089/cell.2009.0060) PMID: [20436954](https://pubmed.ncbi.nlm.nih.gov/20436954/)
7. Biernaskie J, Miller F(2006) Skin-derived precursors(SKPs): *In vivo* cell fate is limited to the neural crest lineage, and is determined by tissue-specific factors. *Int J Devl Neuroscience* 24: 514.
8. Biernaskie J, Paris M, Morozova O, Fagan BM, Marra M, et al(2009) SKPs derive from hair follicle precursors and exhibit properties of adult dermal stem cells. *Cell Stem Cell* 5: 610–623. doi: [10.1016/j.stem.2009.10.019](https://doi.org/10.1016/j.stem.2009.10.019) PMID: [19951689](https://pubmed.ncbi.nlm.nih.gov/19951689/)
9. Cloonan N, Forrest AR, Kolle G, Gardiner BB, Faulkner GJ, et al(2008) Stem cell transcriptome profiling via massive-scale mRNA sequencing. *Nat Methods* 5: 613–619. doi: [10.1038/nmeth.1223](https://doi.org/10.1038/nmeth.1223) PMID: [18516046](https://pubmed.ncbi.nlm.nih.gov/18516046/)
10. Mortazavi A, Williams BA, McCue K, Schaeffer L, Wold B(2008) Mapping and quantifying mammalian transcriptomes by RNA-Seq. *Nat Methods* 5: 621–628. doi: [10.1038/nmeth.1226](https://doi.org/10.1038/nmeth.1226) PMID: [18516045](https://pubmed.ncbi.nlm.nih.gov/18516045/)
11. Trapnell C, Williams BA, Pertea G, Mortazavi A, Kwan G, et al(2010) Transcript assembly and quantification by RNA-Seq reveals unannotated transcripts and isoform switching during cell differentiation. *Nat Biotechnol* 28: 511–515. doi: [10.1038/nbt.1621](https://doi.org/10.1038/nbt.1621) PMID: [20436464](https://pubmed.ncbi.nlm.nih.gov/20436464/)
12. Guttman M, Garber M, Levin JZ, Donaghey J, Robinson J, et al(2010) Ab initio reconstruction of cell type-specific transcriptomes in mouse reveals the conserved multi-exonic structure of lincRNAs. *Nat Biotechnol* 28: 503–510. doi: [10.1038/nbt.1633](https://doi.org/10.1038/nbt.1633) PMID: [20436462](https://pubmed.ncbi.nlm.nih.gov/20436462/)
13. Wilhelm BT, Landry JR(2009) RNA-Seq quantitative measurement of expression through massively parallel RNA-sequencing. *Methods* 48: 249–257. doi: [10.1016/j.ymeth.2009.03.016](https://doi.org/10.1016/j.ymeth.2009.03.016) PMID: [19336255](https://pubmed.ncbi.nlm.nih.gov/19336255/)
14. Marioni JC, Mason CE, Mane SM, Stephens M, Gilad Y(2008) RNA-seq: An assessment of technical reproducibility and comparison with gene expression arrays. *Genome Res* 18: 1509–1517. doi: [10.1101/gr.079558.108](https://doi.org/10.1101/gr.079558.108) PMID: [18550803](https://pubmed.ncbi.nlm.nih.gov/18550803/)
15. Fu X, Fu N, Guo S, Yan Z, Xu Y, et al(2009) Estimating accuracy of RNA-seq and microarrays with proteomics. *BMC Genomics* 10: 161. doi: [10.1186/1471-2164-10-161](https://doi.org/10.1186/1471-2164-10-161) PMID: [19371429](https://pubmed.ncbi.nlm.nih.gov/19371429/)
16. Biernaskie JA, McKenzie IA, Toma JG, Miller FD(2006) Isolation of skin-derived precursors(SKPs) and differentiation and enrichment of their Schwann cell progeny. *Nat Protoc* 1: 2803–2812. PMID: [17406538](https://pubmed.ncbi.nlm.nih.gov/17406538/)
17. Li R, Yu C, Li Y, Lam TW, Yiu SM, et al(2009) SOAP2: An improved ultrafast tool for short read alignment. *Bioinformatics* 25: 1966–1967. doi: [10.1093/bioinformatics/btp336](https://doi.org/10.1093/bioinformatics/btp336) PMID: [19497933](https://pubmed.ncbi.nlm.nih.gov/19497933/)
18. Audic S, Claverie JM(1997) The significance of digital gene expression profiles. *Genome Res* 7: 986–995. PMID: [9331369](https://pubmed.ncbi.nlm.nih.gov/9331369/)
19. Benjamini Y, Yekutieli D(2001) The control of the false discovery rate in multiple testing under dependency. *Ann Stat* 29: 1165–1188.
20. Ye J, Fang L, Zheng H, Zhang Y, Chen J, et al(2006) WEGO: a web tool for plotting GO annotations. *Nucleic Acids Res* 34: W293–297. PMID: [16845012](https://pubmed.ncbi.nlm.nih.gov/16845012/)
21. Kanehisa M, Araki M, Goto S, Hattori M, Hirakawa M, et al(2008) KEGG for linking genomes to life and the environment. *Nucleic Acids Res* 36: D480–484. PMID: [18077471](https://pubmed.ncbi.nlm.nih.gov/18077471/)
22. Wolfe A, Thomas A, Edwards G, Jaseja R, Guo GL, et al(2011) Increased activation of the Wnt/ β -catenin pathway in spontaneous hepatocellular carcinoma observed in farnesoid X receptor knockout mice. *J Pharmacol Exp Ther* 338: 12–21. doi: [10.1124/jpet.111.179390](https://doi.org/10.1124/jpet.111.179390) PMID: [21430080](https://pubmed.ncbi.nlm.nih.gov/21430080/)
23. Hammarstedt A, Hedjazifar S, Jenndahl L, Gogg S, Grünberg J, et al(2013) WISP2 regulates preadipocyte commitment and PPAR γ activation by BMP4. *Proc Natl Acad Sci U S A* 110: 2563–2568. doi: [10.1073/pnas.1211255110](https://doi.org/10.1073/pnas.1211255110) PMID: [23359679](https://pubmed.ncbi.nlm.nih.gov/23359679/)
24. Bige N, Shweke N, Benhassine S, Jouanneau C, Vandermeersch S, et al(2012) Thrombospondin-1 plays a profibrotic and pro-inflammatory role during ureteric obstruction. *Kidney Int* 81: 1226–1238. doi: [10.1038/ki.2012.21](https://doi.org/10.1038/ki.2012.21) PMID: [22418977](https://pubmed.ncbi.nlm.nih.gov/22418977/)
25. Pallero MA, Elzie CA, Chen J, Mosher DF, Murphy-Ullrich JE(2008) Thrombospondin 1 binding to calreticulin-LRP1 signals resistance to anoikis. *FASEB J* 22: 3968–3979. doi: [10.1096/fj.07-104802](https://doi.org/10.1096/fj.07-104802) PMID: [18653767](https://pubmed.ncbi.nlm.nih.gov/18653767/)
26. Lee SH, Rho J, Jeong D, Sul JY, Kim T, et al(2006) v-ATPase V0 subunit d2-deficient mice exhibit impaired osteoclast fusion and increased bone formation. *Nat Med* 12: 1403–1409. PMID: [17128270](https://pubmed.ncbi.nlm.nih.gov/17128270/)
27. Satokata I, Maas R(1994) Msx1 deficient mice exhibit cleft palate and abnormalities of craniofacial and tooth development. *Nat Genet* 6: 348–356. PMID: [7914451](https://pubmed.ncbi.nlm.nih.gov/7914451/)
28. Katayama K, Yamada K, Ornathanalai VG, Inoue T, Ota M, et al(2010) Slitrk1-deficient mice display elevated anxiety-like behavior and noradrenergic abnormalities. *Mol Psychiatry* 15: 177–184. doi: [10.1038/mp.2008.97](https://doi.org/10.1038/mp.2008.97) PMID: [18794888](https://pubmed.ncbi.nlm.nih.gov/18794888/)

29. Murakami K, Jiang YP, Tanaka T, Bando Y, Mitrovic B, et al(2013) In vivo analysis of kallikrein-related peptidase 6(KLK6) function in oligodendrocyte development and the expression of myelin proteins. *Neuroscience* 236: 1–11. doi: [10.1016/j.neuroscience.2012.12.073](https://doi.org/10.1016/j.neuroscience.2012.12.073) PMID: [23376368](https://pubmed.ncbi.nlm.nih.gov/23376368/)
30. Ichiki T, Labosky PA, Shiota C, Okuyama S, Imagawa Y, et al(1995) Effects on blood pressure and exploratory behaviour of mice lacking angiotensin II type-2 receptor. *Nature* 377: 748–750. PMID: [7477267](https://pubmed.ncbi.nlm.nih.gov/7477267/)
31. Hein L, Barsh GS, Pratt RE, Dzau VJ, Kobilka BK(1995) Behavioural and cardiovascular effects of disrupting the angiotensin II type-2 receptor in mice. *Nature* 377: 744–747. PMID: [7477266](https://pubmed.ncbi.nlm.nih.gov/7477266/)
32. Gómez-Nicola D, Valle-Argos B, Pallas-Bazarra N, Nieto-Sampedro M(2011) Interleukin-15 regulates proliferation and self-renewal of adult neural stem cells. *MolBiol Cell* 22: 1960–1970.
33. Piccini M, Vitelli F, Seri M, Galiotta LJ, Moran O, et al(1999) KCNE1-like gene is deleted in AMME contiguous gene syndrome: identification and characterization of the human and mouse homologs. *Genomics* 60: 251–257. PMID: [10493825](https://pubmed.ncbi.nlm.nih.gov/10493825/)
34. Benner EJ, Luciano D, Jo R, Abdi K, Paez-Gonzalez P, et al(2013) Protective astrogenesis from the SVZ niche after injury is controlled by Notch modulator Thbs4. *Nature* 497: 369–373. doi: [10.1038/nature12069](https://doi.org/10.1038/nature12069) PMID: [23615612](https://pubmed.ncbi.nlm.nih.gov/23615612/)
35. Kitisin K, Saha T, Blake T, Golestaneh N, Deng M, et al(2007) Tgf-Beta signaling in development. *Sci STKE* 2007: cm1.
36. Massagué J, Xi Q(2012) TGF- β control of stem cell differentiation genes. *FEBS Lett* 586: 1953–1958. doi: [10.1016/j.febslet.2012.03.023](https://doi.org/10.1016/j.febslet.2012.03.023) PMID: [22710171](https://pubmed.ncbi.nlm.nih.gov/22710171/)
37. Sinha S, Hoofnagle MH, Kingston PA, McCanna ME, Owens GK(2004) Transforming growth factor-beta1 signaling contributes to development of smooth muscle cells from embryonic stem cells. *Am J Physiol Cell Physiol* 287: C1560–1568. PMID: [15306544](https://pubmed.ncbi.nlm.nih.gov/15306544/)
38. Yang Z, Sui L, Toh WS, Lee EH, Cao T(2009) Stage-dependent effect of TGF-beta1 on chondrogenic differentiation of human embryonic stem cells. *Stem Cells Dev* 18: 929–940. doi: [10.1089/scd.2008.0219](https://doi.org/10.1089/scd.2008.0219) PMID: [18855519](https://pubmed.ncbi.nlm.nih.gov/18855519/)
39. Falk S, Joosten E, Kaartinen V, Sommer L(2013) Smad4 and Trim33/Tif1y Redundantly Regulate Neural Stem Cells in the Developing Cortex. *Cereb Cortex* 24: 2951–2963. doi: [10.1093/cercor/bht149](https://doi.org/10.1093/cercor/bht149) PMID: [23765158](https://pubmed.ncbi.nlm.nih.gov/23765158/)
40. Liu DD, Zhang JC, Zhang Q, Wang SX, Yang MS(2013) TGF- β /BMP signaling pathway is involved in cerium-promoted osteogenic differentiation of mesenchymal stem cells. *J Cell Biochem* 114: 1105–1114. doi: [10.1002/jcb.24451](https://doi.org/10.1002/jcb.24451) PMID: [23150386](https://pubmed.ncbi.nlm.nih.gov/23150386/)
41. Liu Y, Zheng WK, Gao WS, Shen Y, Ding WY(2013) Function of TGF-beta and p38 MAKP signaling pathway in osteoblast differentiation from rat adipose-derived stem cells. *Eur Rev Med Pharmacol Sci* 17: 1611–1619. PMID: [23832727](https://pubmed.ncbi.nlm.nih.gov/23832727/)
42. Feng Z, Srivastava AS, Mishra R, Carrier E(2004) A regulatory role of Wnt signaling pathway in the hematopoietic differentiation of murine embryonic stem cells. *Biochem Biophys Res Commun* 324: 1333–1339. PMID: [15504360](https://pubmed.ncbi.nlm.nih.gov/15504360/)
43. Chen BY, Wang X, Wang ZY, Wang YZ, Chen LW, et al(2013) Brain-derived neurotrophicfactor stimulates proliferation and differentiation of neural stem cells, possibly by triggering the Wnt/ β -catenin signaling pathway. *J Neurosci Res* 91: 30–41. doi: [10.1002/jnr.23138](https://doi.org/10.1002/jnr.23138) PMID: [23023811](https://pubmed.ncbi.nlm.nih.gov/23023811/)
44. Zhang LL, Liu JJ, Liu F, Liu WH, Wang YS, et al(2012) MiR-499 induces cardiac differentiation of rat mesenchymal stem cells through wnt/ β -catenin signaling pathway. *Biochem Biophys Res Commun* 420: 875–881. doi: [10.1016/j.bbrc.2012.03.092](https://doi.org/10.1016/j.bbrc.2012.03.092) PMID: [22465011](https://pubmed.ncbi.nlm.nih.gov/22465011/)
45. Plescia C, Rogler C, Rogler L(2001) Genomic expression analysis implicates Wnt signaling pathway and extracellular matrix alterations in hepatic specification and differentiation of murine hepatic stem cells. *Differentiation* 68: 254–269. PMID: [11776478](https://pubmed.ncbi.nlm.nih.gov/11776478/)
46. Yang W, Yan HX, Chen L, Liu Q, He YQ, et al(2008) Wnt/beta-catenin signaling contributes to activation of normal and tumorigenic liver progenitor cells. *Cancer Res* 68: 4287–4295. doi: [10.1158/0008-5472.CAN-07-6691](https://doi.org/10.1158/0008-5472.CAN-07-6691) PMID: [18519688](https://pubmed.ncbi.nlm.nih.gov/18519688/)
47. Ke Z, Mao X, Li S, Wang R, Wang L, et al(2012) Dynamic expression characteristics of Notch signal in bone marrow-derived mesenchymal stem cells during the process of differentiation into hepatocytes. *Tissue Cell* 45: 95–100. doi: [10.1016/j.tice.2012.09.008](https://doi.org/10.1016/j.tice.2012.09.008) PMID: [23116754](https://pubmed.ncbi.nlm.nih.gov/23116754/)
48. Osathanon T, Subbalekha K, Sastravaha P, Pavasant P(2012) Notch signalling inhibits the adipogenic differentiation of single-cell-derived mesenchymal stem cell clones isolated from human adipose tissue. *Cell Biol Int* 36: 1161–1170. doi: [10.1042/CBI20120288](https://doi.org/10.1042/CBI20120288) PMID: [22974058](https://pubmed.ncbi.nlm.nih.gov/22974058/)